[2]R. J. Elliott, Phys. Rev. 124, 340 (1961); see also R. J. Elliott, in *Polarons and Excitons*, edited by C. G. Kuper and G. D. Whitfield (Oliver and Boyd, London, 1963), p. 269.
[3]F. Pradère, B. Sacks, and A. Mysyrowicz, Opt. Commun. 1, 234 (1969).
[4]R. Loudon, Proc. Phys. Soc. (London) 80, 952 (1962).
[5]G. D. Mahan, Phys. Rev. 170, 825 (1968).
[6]S. N. Shestatskii, V. V. Sobolev, and N. P. Likhobabin, Phys. Status Solidi 42, 669 (1970).
[7]U. Fano, Phys. Rev. 124, 1866 (1961).
[8]The configuration mixing in the case of excitonic bound states degenerate with a continuum of states has been considered earlier. See, e.g., D. L. Greenaway and G. Harbeke, *Optical Properties and Band Structure of Semiconductors* (Pergamon, New York, 1968), Chap. 8.

PHYSICAL REVIEW B VOLUME 4, NUMBER 10 15 NOVEMBER 1971

Far-Infrared Optical Constants of KI†

J. I. Berg* and E. E. Bell
Department of Physics, The Ohio State University, Columbus, Ohio 43210
(Received 14 May 1971)

The far-infrared optical constants of KI were studied in the vicinity of the TO($\vec{k}=0$) phonon frequency $\nu_0 = 101$ cm^{-1} (in wave-number units). Experimental values of the optical constants at $T = 300\,^\circ$K were determined from transmission and reflection measurements employing a Michelson interferometer operated in the asymmetric mode. Theoretical values were calculated from a theory which utilizes thermodynamic Green's functions to include the effects of the interaction of the optically active phonon with other phonons because of cubic anharmonicity. Phonon-dispersion data for the calculation were generated from a shell model, with parameters selected by Dolling to give the phonon frequencies as determined from neutron-diffraction experiments. Good agreement for the optical constants in the region approximately 20–175 cm^{-1} was obtained by using a nearest-neighbor central-force model and adjusting the third derivative of the K^+-I^- bond potential to $\Phi'''(r_0) = -3.6\times10^{12}$ erg/cm^3.

I. INTRODUCTION

The dominant interaction of infrared radiation in cubic ionic diatomic crystals is with the TO lattice-vibrational mode of the same wave vector $\vec{k}$ as the incident electromagnetic wave and with polarization in the electric field direction. This interaction results in the fundamental absorption band or reststrahl band, characterized by very high absorption and reflection in the neighborhood of the TO($\vec{k}=0$) phonon frequency or "eigenfrequency" ν_0 ("frequency" here measured in wave-number units cm^{-1}). To account for the detailed shape of the band, one must consider the dampening effect of the anharmonic parts of the interionic forces on the optically active vibrational mode. Theoretical studies of this effect have been carried out by Cowley,[1] Gurevich and Ipatova,[2] and Wallis, Ipatova, and Maradudin.[3] These authors, using theromodynamic Green's-function techniques, have derived expressions for the lattice contribution to the complex dielectric susceptibility. Their expressions differ from that calculated on the basis of a purely harmonic model in that a complex self-energy term is added to the denominator. This term expresses the effect of three- and four-phonon interactions due to cubic and quartic terms in the anharmonic potential, respectively.

In view of the theoretical effort mentioned above, the availability of phonon-dispersion data for many crystals of the NaCl structure type, and recent advances in far-infrared spectroscopy, we have undertaken detailed measurements of the optical constants n and k, the index of refraction and the extinction coefficient, respectively, of some of these crystals in the neighborhood of their eigenfrequencies. The results for KCl and KBr have already been published.[4] In this paper we present the experimental results for KI at $T = 300\,^\circ$K, along with a calculation of the optical constants including only the effects of cubic anharmonicity. KI was chosen because of the availability of phonon-dispersion data based on actual neutron-diffraction experiments[5] at 77 °K and because its absorption band falls in the optimum region for employment of the experimental technique used in this work. The room-temperature eigenfrequency of KI is $\nu_0 = 101$ cm^{-1}.

The optical constants were determined from transmission and reflection experiments using a Michelson interferometer operated in the asymmetric mode, as described by Bell[6] and by Russell and Bell.[7] In the asymmetric mode the sample is placed in one of the arms of the interferometer. With the sample removed from its position, an interferogram, or detector signal as a function of

optical-path difference between the arms, is taken.

This interferogram is symmetric about the "white-light" peak which occurs at zero optical-path difference. With the sample in place the interferogram becomes asymmetric. By comparing the complex Fourier transforms of the sample and "background" interferograms, the relative amplitude and phase of each spectral component as affected by the sample can be determined. From the amplitude and phase the real and imaginary parts of the complex index of refraction $\hat{n} = n + ik$ can be computed. The technique thus has an advantage over conventional power spectroscopy, where only the square of the relative amplitude is measured and dispersion relations must be used to obtain phase information. The technique is limited to longer wavelengths, however, owing to the sensitivity, particularly of the amplitude, to various possible deviations from ideal sample and instrument geometry. In this work reliable phase information could be taken at frequencies as high as 700 cm^{-1}, while the high-frequency limit for reliable amplitude information was considerably lower, depending upon the sample used. The low-frequency limit, approximately 20 cm^{-1}, was set by the spectral distribution of emission from the high-pressure Hg arc used as a source of radiation.

In the calculation presented here, the theoretical development of Cowley[1] was followed closely. On the basis of a quasiharmonic approximation, where the Hamiltonian is renormalized at each temperature, Cowley derives an expression for the dielectric susceptibility in terms of a thermodynamic Green's function. The renormalized frequencies for any temperature $T > 0$ correspond to the peaks in the infrared or inelastic neutron scattering spectra. Using the shell model of Dolling *et al.*[5] and readjusting certain force constants to account for the temperature difference between that of their experiment and that of ours, we have computed the frequencies and polarizations of phonons for $\vec{k}$ values at the 1000 points in the Brillouin zone generated from the 48 points in an irreducible element of the zone originally chosen by Kellerman.[6] With this eigendata sample, we have calculated the self-energy and the optical constants. Only the anharmonicity in the nearest-neighbor bonds was included. Four parameters were adjusted to give agreement with experiment. They are the limiting dielectric constants $\epsilon(0)$ and $\epsilon(\infty)$, the eigenfrequency ν_0, and the third derivative with respect to the nearest-neighbor separation distance r of the K^+-I^- bond potential $\Phi(r)$, evaluated at the equilibrium point $r = r_0$.

II. EXPERIMENTAL

To determine the optical constants of KI, transmission experiments were performed on lamellar samples as thin as 100 μm, while reflection experiments were performed on much thicker (approximately 1 cm) samples having only one lapped and polished surface. The reflection samples were prepared as described by Johnson and Bell.[4] Transmission samples with optically usable circular regions as large as $\frac{3}{4}$ in. in diameter were prepared in the following manner. After lapping and polishing one surface of a relatively thick cylindrical piece of crystalline KI obtained from the Harshaw Chemical Company, the prepared surface was fastened with an Epoxy cement to a brass plate with a $\frac{3}{4}$-in.-diameter hole at the center. The brass plate was then secured with screws to the inner-end surface of a two-part cylindrical sample holder for lapping of the other side of the sample. The outer-end surface of the sample holder then served as an adjustable reference plane determining the thickness of the sample. During this operation the hole was filled by a brass disk of precisely the thickness of the brass plate for support of the region of the sample to be used for optical transmission. After preparation the sample was retained on the brass plate and could be handled easily without danger of cracking. As discussed below, it is important that the spread in thickness across the face of the sample be minimized for use in amplitude spectroscopy. Although care was taken to keep the surfaces parallel, variations in thickness of a few μm were difficult to avoid.

Although reflection measurements alone can be used in principle to determine the optical constants, practical difficulties in placement of the sample for reflection can cause an error in the phase.[4] On the other hand, the thinnest KI transmission samples we were able to prepare had an opaque region from approximately 90 to 160 cm^{-1} (see Fig. 1). Using the values of the optical constants measured in transmission in the wings of the absorption region, the uncertainty in the absolute phase in the reflection measurements was removed. Thus the reflection measurements could be used in the region opaque to transmission. Amplitude spectroscopy was also used to advantage in approaching the eigenfrequency in transmission. That is, since the detector responds to amplitude rather than power reduction, the equivalent absorption coefficient measurement by power spectroscopy would require a sample half as thick.

To employ digital techniques in computation of the Fourier transforms of the interferograms, detector power $P(x)$ was measured for a finite number of evenly spaced values of the optical path x. For an optical-path increment Δx, the maximum frequency which can be included in the spectrum for an unambiguous Fourier transform is $\nu_{max} = (2\Delta x)^{-1}$. The sampling interval X, a finite multiple of Δx, determines the resolution $\Delta\nu = 2/X$[6].

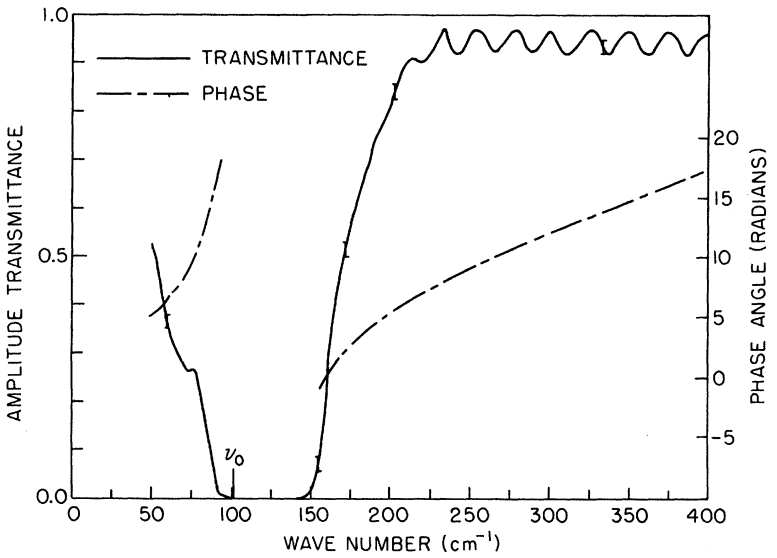

FIG. 1. Amplitude transmittance g_t and phase ϕ_t for a 115.2-μm-thick KI sample. The resolution is $\Delta\nu = 5$ cm^{-1}. The vertical bars indicate approximate error ranges.

Although Δx and X for background and sample interferograms were chosen to be identical, the center of the measuring interval for the sample interferogram was sometimes shifted forward by an optical-path length L with respect to that of the background interferogram, as discussed below.

The basic relationship between the complex Fourier transform $\hat{p}_1$ of the background interferogram and that of the sample interferogram $\hat{p}_2$ (the frequency dependence is implicit) is[6]

$$\hat{p}_2 = \hat{g}\hat{p}_1 , \tag{1}$$

where $\hat{g} = g e^{i\phi}$ is the Fourier transform of the impulse response function of the sample. This depends upon the geometry of the sample and the mode of measurement. For reflection from a single surface, where the background interferogram is taken with a mirror in place of the sample,

$$\hat{g}_r = -\hat{r} , \tag{2}$$

where $\hat{r}$ is the complex amplitude reflectivity of the sample, $\hat{r} = (1-\hat{n})/(1+\hat{n})$. For transmission, where the background interferogram is taken with the sample simply removed,[6]

$$\hat{g}_t = \hat{t} e^{-2\pi i\nu b} = (1-\hat{r}^2)\sum_{l=0}^{\infty} \hat{r}^{2l} e^{2\pi i\nu b[(2l+1)\hat{n}-1]} . \tag{3}$$

Here $\hat{t}$ is the complex amplitude transmittance and b is the sample thickness. The function $\hat{g}$ also may contain a factor $e^{-2\pi i\nu L}$, where L is the arbitrary optical-path shift chosen to "center" the sample interferogram in the case of transmission, or an unwanted and unpredictable value of the order of a few μm due to errors in mirror-sample interchangeability in the case of reflection. Equation (3) for transmission is in the form of a series of partial waves, the higher orders of which are the familiar channeled spectrum due to multiple reflections between the surfaces. The interferogram for each term is then roughly an "echo" of the background interferogram, the lth echo being displaced an optical-path distance $b[(2l+1)n-1]$ from the center of the background interferogram (with $L=0$). Owing to the finite sampling interval X, the higher orders beyond some value l_m will not be included in the measured sample interferogram, so that the series (3) can be terminated at $l = l_m$. For the present values of b and n and the resolution $\Delta\nu = 5$ cm^{-1}, l_m was never greater than 2.

Since the detector in the asymmetric interferometer responds to the relative amplitude of radiation integrated across the face of a transmission sample, a variation in thickness across this face causes a variation in the phase, resulting in a reduction in the integrated amplitude. For a given frequency ν, the effect will be serious for order l provided $\Delta b \gtrsim \{\nu[(2l+1)n-1]\}^{-1}$, where Δb is the average spread in thickness. We corrected for this effect using the correction factor[9]

$$\hat{\delta}_l = \frac{\sin\{\pi\nu\Delta b[(2l+1)\hat{n}-1]\}}{\pi\nu\Delta b[(2l+1)\hat{n}-1]} \tag{4}$$

for each term in (3). The parameter Δb was determined for each sample from the decrease in channeled spectrum amplitude with frequency in the high-frequency region of low absorption. This Δb was then used in the computation of $\hat{n}$ at lower frequencies.

Since (3) cannot be solved explicitly for $\hat{n}$ in terms of $\hat{g}_t$, a spectral point-by-point iterative procedure was developed for a computer calculation. The complex index $\hat{n}$ was evaluated at each point from the value of the argument of the exponential in the $l=0$ term, this argument being computed by using trial values of $\hat{n}$ in the remaining parts dependent upon $\hat{n}$. Since the imaginary part of the argument (the phase) is only defined modulo 2π, the calculation for the initial point in a given spectral interval was chosen to give the most reasonable value of n, while the phase cycle for succeeding points was chosen to assure continuity of n.

In the absence of other methods for determining the average thickness of our very fragile samples to the desired accuracy, we used the known index values[10] in the region approximately 340–630 cm^{-1} to determine the thickness b_0 for each sample which would give these index values in this region by our technique. Figure 1 shows the amplitude transmittance g_t and phase ϕ_t for a sample for which $b_0 = 119.2 \pm 0.5$ μm and $\Delta b = 3.0 \pm 1.0$ μm. The presence of channeled spectrum out to 400 cm^{-1} is indicative of a relatively high-quality sample. Note that the channeled spectrum in the phase function is too small to be seen on the scale of Fig. 1.

Figure 2 shows the power reflectance g_r^2 (obtained by squaring our amplitude reflectivity values) and the phase ϕ_r averaged from several measurements on two reflection samples. Figure 3 shows the very low reflectance values in greater detail. The mirror-sample optical-path difference was evaluated using the optical constants determined in transmission at $\nu = 85$ cm^{-1}. It is significant to note that the Kramers-Kronig analysis of Hadni *et al.*[11] based on power spectroscopic measurements with resolution apparently at least as great as that used here failed to reveal any of the structure shown at the phase peak in Fig. 2. The power reflectance here shows no definite structure in the region of the very noticeable structure in the phase near 155 cm^{-1}, indicating that higher accuracy would be needed to obtain this structure from the power reflectance alone.

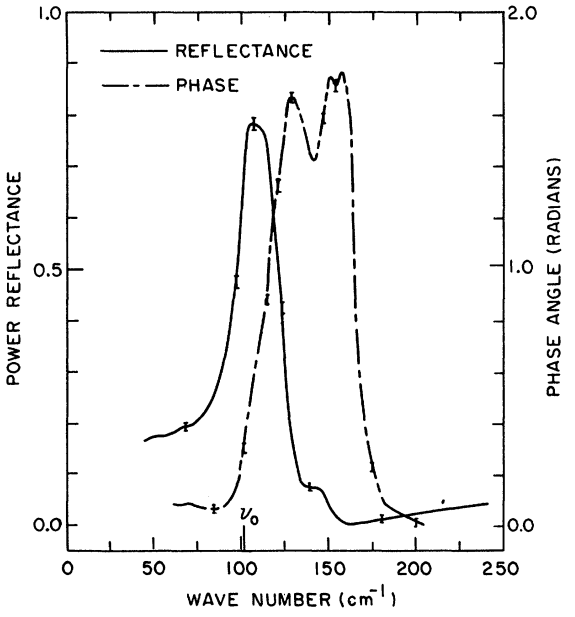

FIG. 2. Power reflectance g_r^2 and the phase ϕ_r averaged from measurements on two polished samples of KI.

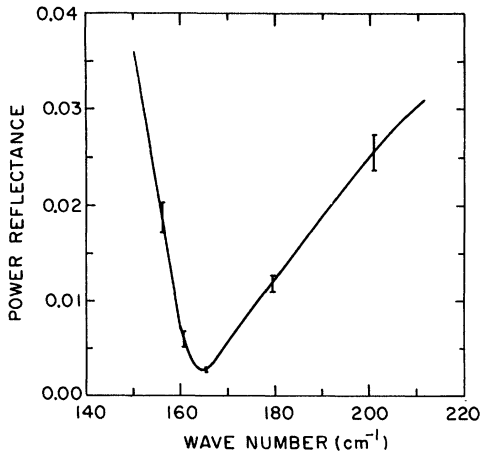

FIG. 3. Power reflectance g_r^2 of KI in the region of very low reflectance.

In Fig. 4 we summarize the results of determination of the optical constants of KI from several transmission and reflection experiments. The asymmetric technique was used for all values except the values of k in the region $\nu > 190$ cm^{-1}, where a conventional power transmission experiment was carried out on a 700-μm-thick sample. This was done because of unreliable amplitude data for a sample this thick at the higher frequencies. Using the linear dependence of n on ν^2 in the low-frequency limit, an extrapolation to $\nu = 0$ was made, as shown in Fig. 5. The value so determined, $n(0) = 2.24 \pm 0.01$, gives a zero-frequency dielectric constant of $\epsilon(0) = n^2(0) = 5.02 \pm 0.04$. Reported values of the static dielectric constants ϵ_s range from 4.94 to 5.09.[12–15] The structure shown here near 40 cm^{-1}, not visible in Fig. 4, is evidently associated with the structure in the extinction coefficient below the eigenfrequency. The relatively easily obtained and accurate values of the index of refraction in this spectral region can be attributed to the ability of the asymmetric technique to yield phase information in a transmission experiment.

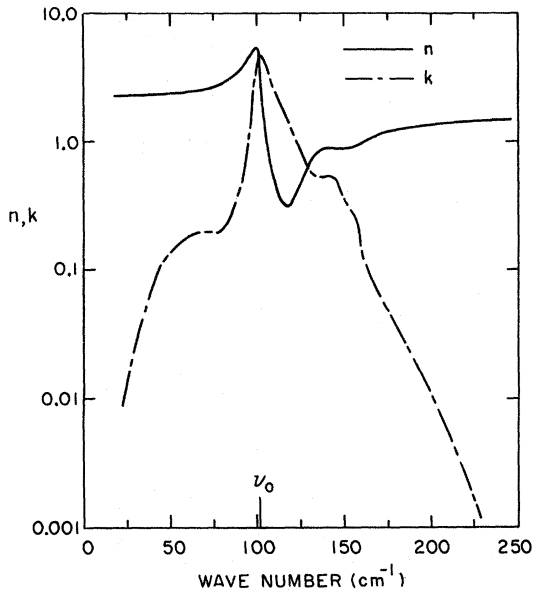

FIG. 4. Optical constants n and k of KI determined from transmission and reflection measurements.

III. THEORETICAL

Using the expression derived by Cowley[1] for the ionic contribution to the complex dielectric susceptibility for cubic crystals, and the elementary formula of electromagnetic theory $\hat{n}^2=\hat{\epsilon}$, where $\hat{\epsilon}$ is the complex dielectric constant, we obtain

$$\hat{n}^2(\omega)=\epsilon(\infty)+\frac{[\epsilon(0)-\epsilon(\infty)][\omega_0^2+2\omega_0\Delta(0j_0,0)]}{\omega_0^2-\omega^2+2\omega_0[\Delta(0j_0,\omega)-i\Gamma(0j_0,\omega)]}\,. \tag{5}$$

The symbol ω is used for angular frequencies, $\omega=2\pi c\nu$. The bracketed quantity in the denominator of (5) is the renormalized self-energy of the TO(0) mode, divided by $\hbar$. The TO(0) mode here is specified by wave vector $\vec{k}=0$ and a branch index $j=j_0$. The real part $\Delta(0j_0,\omega)$ of this complex function is the frequency shift and the negative imaginary part $\Gamma(0j_0,\omega)$ is the inverse lifetime of the $0j_0$ mode. Since the inverse lifetime vanishes in the low- and high-frequency limits, $n^2(0)=\epsilon(0)$ and $n^2(\infty)=\epsilon(\infty)$, the high-frequency dielectric constant being greater than unity due to all processes resonating above ω_0. Taking $\omega_0\equiv\omega(0j_0)$ as the quasiharmonic eigenfrequency for the temperature $T>0$ rather than the true harmonic eigenfrequency requires that the real part of the self-energy, now the renormalized self-energy, vanish at $\omega=\omega_0$.[4] Here we compute only the frequency-dependent parts of the self-energy, adjusting the sum of all frequency-independent parts of the frequency shift such that the total frequency shift vanishes at ω_0. To limit the complexity of the calculation we consider only that part due to cubic anharmonicity.

The cubic part of the anharmonic Hamiltonian can be expressed as

$$H_3=\sum_{\vec{k}_1 j_1}\sum_{\vec{k}_2 j_2}\sum_{\vec{k}_3 j_3} V(\vec{k}_1 j_1,\vec{k}_2 j_2,\vec{k}_3 j_3)\times A(\vec{k}_1 j_1)A(\vec{k}_2 j_2)A(\vec{k}_3 j_3)\,, \tag{6}$$

where the operators $A(\vec{k}j)$ are linear combinations of creation and annihilation operators, $A(\vec{k}j)=a(\vec{k}j)+a^\dagger(-\vec{k}j)$.[16] The potential-energy coefficients $V(\vec{k}_1 j_1,\vec{k}_2 j_2,\vec{k}_3 j_3)$ can be found from the coefficients for the Taylor-series expansion of the potential energy in terms of the ionic vibrational coordinates $u_\alpha(KL)$. Here α is a Cartesian index, K numbers the ions within a unit cell, $K=1$ or 2, and L numbers the unit cells, $L=0,1,\ldots,N-1$, where N is the number of unit cells in the crystal. The transformation is[16]

$$u_\alpha(KL)=\sum_{\vec{k}j}^{6N}\left(\frac{\hbar}{2NM_K\omega(\vec{k}j)}\right)^{1/2} m_\alpha(K|\vec{k}j)\times e^{i\vec{k}\cdot(\vec{r}_K+\vec{r}_L)}A(\vec{k}j)\,. \tag{7}$$

In this expression M_K is the mass of the Kth ion, $m_\alpha(K|\vec{k}j)$ is a real eigenvector component, $\vec{r}_K$ is a vector from the origin of the unit cell to the Kth ion, and $\vec{r}_L$ is a vector from the origin of the $L=0$ unit cell to that of the Lth unit cell. We will not write the expression for the most general potential-energy coefficient, since we are only interested in

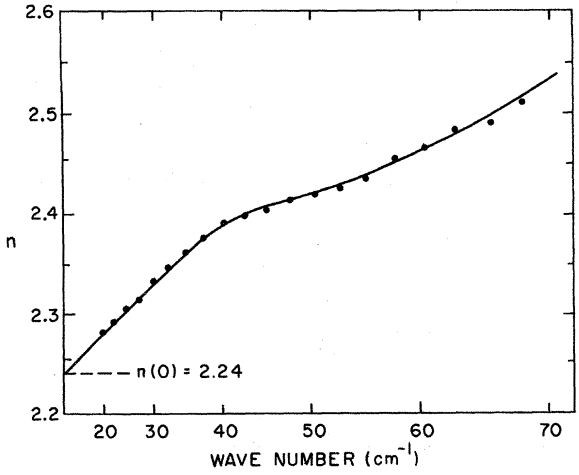

FIG. 5. Index of refraction n of KI in the low-frequency region obtained from transmission measurements. The abscissa is proportional to the square of frequency.

a special case, as discussed below. We note here that this coefficient vanishes unless $\vec{k}_1+\vec{k}_2+\vec{k}_3=\vec{G}$, where $\vec{G}$ is a reciprocal-lattice vector.[17] This leads to conservation of wave vector in multiphonon interactions governed by anharmonicity.

The third-order frequency-dependent contribution to the self-energy, using an infinitesimal positive parameter η to avoid singularities in the usual manner for Fourier transforms, is[1,18]

$$D_3(0j_0,\omega)=-\frac{18}{\hbar}\sum_{\vec{k}_1 j_1}\sum_{\vec{k}_2 j_2}|V(0j_0,\vec{k}_1 j_1,\vec{k}_2 j_2)|^2 \times\lim_{\eta\to 0}F(\omega+i\eta)\,. \quad (8)$$

The function $F(\omega)$ is given by

$$F(\omega)=[n(\vec{k}_1 j_1)+n(\vec{k}_2 j_2)+1]\left(\frac{1}{\omega(\vec{k}_1 j_1)+\omega(\vec{k}_2 j_2)+\omega}+\frac{1}{\omega(\vec{k}_1 j_1)+\omega(\vec{k}_2 j_2)-\omega}\right)$$
$$+[n(\vec{k}_1 j_1)-n(\vec{k}_2 j_2)]\left(\frac{1}{\omega(\vec{k}_2 j_2)-\omega(\vec{k}_1 j_1)+\omega}+\frac{1}{\omega(\vec{k}_2 j_2)-\omega(\vec{k}_1 j_1)-\omega}\right). \quad (9)$$

Here $n(\vec{k}j)$ is a thermally averaged population number for mode $\vec{k}j$, $n(\vec{k}j)=(e^{\hbar\omega(\vec{k}j)/k_BT}-1)^{-1}$, where k_B is the Boltzmann constant. The frequency shift and inverse lifetime are then given by

$$\Delta(0j_0,\omega)=(1/\hbar)\mathrm{Re}[D_3(0j_0,\omega)-D_3(0j_0,\omega_0)]\,,$$
$$\Gamma(0j_0,\omega)=-(1/\hbar)\mathrm{Im}[D_3(0j_0,\omega)]\,, \quad (10)$$

where Re and Im denote real and imaginary parts, respectively. Owing to conservation of wave vector, the double sum over wave vector in (8) can be reduced to a single sum, since $\vec{k}_1+\vec{k}_2=\vec{G}=0$, where only wave vectors in the first Brillouin zone need be considered. Thus only the coefficient $V(0j_0,\vec{k}j_1,-\vec{k}j_2)$ is needed.

To express the coefficient $V(0j_0,\vec{k}j_1,-\vec{k}j_2)$ in a form suitable for computation, we first define the quantity

$$w_{\alpha\alpha'}(\vec{k}j_1j_2)=[m_\alpha(1|\vec{k}j_1)m_{\alpha'}(2|\vec{k}j_2)+m_{\alpha'}(1|\vec{k}j_1)m_\alpha(2|\vec{k}j_2)]-[m_\alpha(2|\vec{k}j_1)m_{\alpha'}(1|\vec{k}j_2)+m_{\alpha'}(2|\vec{k}j_1)m_\alpha(1|\vec{k}j_2)]\,. \quad (11)$$

Taking the wave vector 0 of the incoming wave in the positive x direction and the wave motion specified by j_0 along the z axis, we find, using the transformation (7), that

$$V(0j_0,\vec{k}j_1,-\vec{k}j_2)=-\frac{i}{3}\left(\frac{\hbar^3}{8NM_1M_2\mu\omega_0\omega(\vec{k}j_1)\omega(\vec{k}j_2)}\right)^{1/2}\times L(zxy,\vec{k}j_1j_2)\,, \quad (12)$$

where μ is the reduced mass $M_1M_2/(M_1+M_2)$ and the coefficient on the right-hand side is defined by

$$L(\alpha\beta\gamma,\vec{k}j_1j_2)=\tfrac{1}{2}\{A_3w_{\alpha\alpha}(\vec{k}j_1j_2)+B_3[w_{\beta\beta}(\vec{k}j_1j_2)+w_{\gamma\gamma}(\vec{k}j_1j_2)]\}\sin(k_\alpha r_0)$$
$$+B_3[w_{\alpha\beta}(\vec{k}j_1j_2)\sin(k_\beta r_0)+w_{\alpha\gamma}(\vec{k}j_1j_2)\sin(k_\gamma r_0)]\,. \quad (13)$$

Here r_0 is the nearest-neighbor equilibrium K^+-I^- separation distance, or half the lattice constant, and the parameters A_3 and B_3 are given in terms of the nearest-neighbor interionic central potential $\Phi(r)$ by

$$A_3=\Phi'''(r_0)\,,$$
$$B_3=(1/r_0)\Phi''(r_0)-(1/r_0^2)\Phi'(r_0)\,. \quad (14)$$

The summation (8) over the entire Brillouin zone can be reduced to a summation over only an irreducible element of the zone by applying the 48 transformations of the full cubic group. One such irreducible element, which was used in the calculation described below, is that such that k_x, k_y, and k_z are all positive, and $k_x>k_y>k_z$. Considering the effect on the eigenvectors $\vec{m}(K|\vec{k}j)$ and subsequently on $V(0j_0,\vec{k}j_1,-\vec{k}j_2)$ given in (12), (11), and (13) resulting from application of the transformations, and using the invariance of the phonon frequencies under these transformations, we find that (8) becomes

$$D_3(0j_0,\omega)=\frac{-4\hbar^2}{N\mu M_1M_2\omega_0}\times\sum_{\vec{k}\,\mathrm{irr}}\sum_{j_1j_2}\sum_\alpha\frac{1}{\omega(\vec{k}j_1)\omega(\vec{k}j_2)}\times L^2(\alpha\beta\gamma,\vec{k}j_1j_2)\lim_{\eta\to0}F(\omega+i\eta)\,, \quad (15)$$

where $\alpha\beta\gamma=xyz$, yzx, or zxy for $\alpha=x$, y, or z, respectively, and $\sum_{\mathrm{irr}}$ denotes summation only over the irreducible element of the zone.

IV. CALCULATION

We consider first the calculation of the frequency-dependent part of the self-energy due to cubic anharmonicity. This is given in Eq. (15) as a sum over phonon wave vector $\vec{k}$ and branch indices j_1 and j_2, where $\vec{k}$ is limited to an irreducible element of the Brillouin zone. To obtain eigenfrequencies $\omega(\vec{k}j)$ and eigenvector components $m_\alpha(K|\vec{k}j)$ to be used in the calculation, the shell model of Woods *et al.*[19] and Cowley *et al.*[20] with parameters selected by Dolling *et al.*[5] was used. The 6×6 Fourier-transformed dynamical matrix[16] for the shell model was computed and diagonalized for $\vec{k}$ values at the 48 evenly spaced points in an irreducible element of the Brillouin zone chosen originally by Kellerman.[8] The complete 11-parameter model of Dolling *et al.* was used. This model includes core and shell charges and core-shell force constants for both ions as well as force constants for nearest-neighbor and next-nearest-neighbor interactions. Since their parameters were selected to give a best fit to frequencies determined by neutron-diffraction experiments at $T=77\,^\circ$K and our experiment was performed at $T=300\,^\circ$K, a slight temperature correction was necessary. The parameters controlling the interionic force constants were multiplied by 0.924, the value necessary to give the room-temperature TO(0) mode frequency correctly, keeping the core-shell force constants and charges constant.

To compute the self-energy, a computer program was written based on (15) with subroutines based on (9) to give the function $F(\omega)$ and on (13) and (11) to give the modified potential-energy coefficient $L(\alpha\beta\gamma,\vec{k}j_1j_2)$. To give a smooth form to the real and imaginary parts, the parameter η was held at 2.5 cm^{-1}. This was large enough to spread the peaks associated with the individual phonon processes using our eigendata sample of 1000 points in the Brillouin zone. Since the half-width of each of the "δ-function" peaks is approximately 2η, the resolution was comparable to that used in the experimental work. In the program, variables were defined for each spectral point, taken 2.5 cm^{-1} apart, so that the contributions for all frequencies for a given coefficient $L(\alpha\beta\gamma,\vec{k}j_1j_2)$ could be found and added to the value of the self-energy already in storage before proceeding to the next $\vec{k}j_1j_2$ combination. The following relation, valid in the $\eta\to0$ limit, was used as a check on our calculation:

$$\int_0^\infty \Gamma(0j_0,\omega)\,d\omega=\frac{-4\pi\hbar}{N\mu M_1M_2\omega_0}$$

$$\times\sum_{\vec{k}\,\mathrm{irr}}\sum_{j_1j_2}\sum_{\alpha} L^2(\alpha\beta\gamma,\vec{k}j_1j_2)\,\frac{1}{\omega(\vec{k}j_1)\omega(\vec{k}j_2)}$$

$$\times\{[n(\vec{k}j_1)+n(\vec{k}j_2)+1]+|n(\vec{k}j_1)-n(\vec{k}j_2)|\}. \quad (16)$$

The summations in the right-hand side of (16) were evaluated along with those in the self-energy (15). Final values of $\Gamma(0j_0,\omega)$ for all of the spectral points were then used to perform a numerical integration to obtain the integral on the left-hand side. The equality was found to hold to better than 2%. Since some of the points selected in the irreducible element of the Brillouin zone are on surfaces of this element and thus correspond to an element of the zone smaller than the $\frac{1}{1000}$ part of the zone in the case of the interior points, a slight modification of (15) and (16) was necessary. Contributions for those points on the boundaries were divided by an appropriate factor, keeping $N=1000$.

Figure 6 shows the frequency shift and inverse lifetime obtained from a calculation of $D_3(0j_0,\omega)$, using (10) to obtain the real and imaginary parts of the renormalized self-energy. The parameters dependent upon the nearest-neighbor potential used in this calculation were $A_3=-3.6\times10^{12}$ erg/cm^3 and $B_3=5.4\times10^{11}$ erg/cm^3. The former was chosen to give agreement with the optical constants, discussed below, while the latter was computed from shell-model data using (14).

The optical constants n and k, compared with experimental values in Figs. 7 and 8, were calculated from the frequency shift and inverse lifetime using

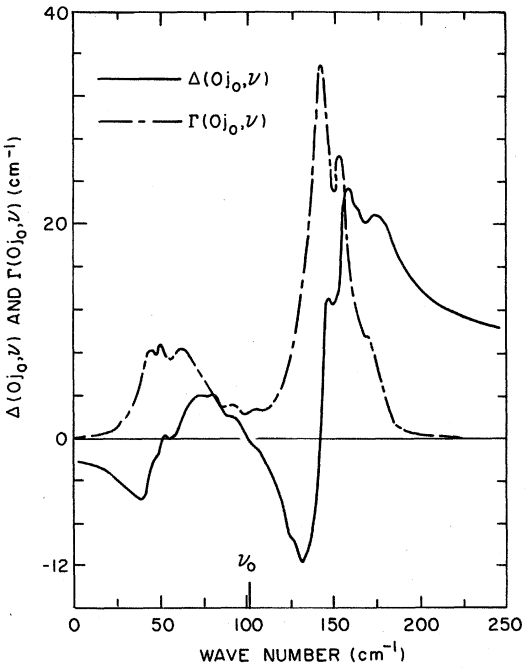

FIG. 6. Calculated frequency shift $\Delta(0j_0,\omega)$ and the inverse lifetime $\Gamma(0j_0,\omega)$ of the TO(0) mode for KI.

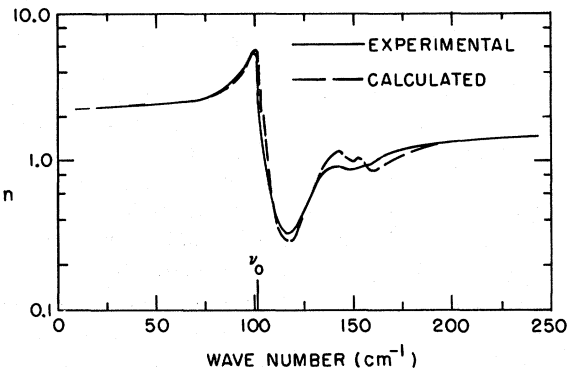

FIG. 7. Experimental and calculated index of refraction for KI.

(5) with the experimentally determined values $\epsilon(0) = 5.02$ (our experiment), $\epsilon(\infty) = 2.69$,[10] and the generally accepted eigenfrequency $\omega_0/2\pi c = 101$ cm^{-1}. The parameter A_3 was chosen to give agreement with our experimental results for k at the eigenfrequency. The value so found was $A_3 = (-3.6 \pm 0.3) \times 10^{12}$ erg/cm^3.

V. DISCUSSION

The general agreement between theory and experiment can be considered quite good. The only drastic disagreement, that for k above 175 cm^{-1}, suggests that the inclusion of quartic anharmonicity would be necessary to give k correctly. This is because the maximum frequency sum for two phonons of the same wave vector $\omega(\vec{k}j_1) + \omega(\vec{k}j_2)$ is around 190 cm^{-1}. We shall return to this point later. The general statement made by other authors[4,21] that agreement in the region above the eigenfrequency is easier to obtain than below the eigenfrequency certainly does not apply to this case. Although part of this may be due to our better experimental values below the eigenfrequency, our method of selecting the parameter $A_3 = \Phi'''(r_0)$ may have a bearing here also.

The method generally used to obtain anharmonic parameters such as our constant A_3 is to assume that the anharmonicity is caused by the short-range repulsive forces alone, then to use a heuristic expression[17] for the potential, such as

$$\Phi(r) = \lambda e^{-r/\rho}, \tag{17}$$

where λ and ρ are determined from experiment. Ipatova *et al.*[21] give a general argument for the neglect of the electrostatic forces in dealing with anharmonicity. Aside from questions of the validity of the expression for the potential, there is the question as to which experimental values should be used to obtain the constants λ and ρ. Using the first and second derivatives derived from the harmonic shell model of Dolling *et al.*,[5] we obtain $A_3 = -6.7 \times 10^{12}$ erg/cm^3, in marked disagreement with our value. From the lattice constant and the compressibility alone, Born and Huang[17] derive values of λ and ρ from which $A_3 = -4.5 \times 10^{12}$ erg/cm^3. It can be verified that if a correction is made to this latter value for the nearest-neighbor electrostatic contribution, good agreement with our value is reached. There is, however, little justification for including only the nearest-neighbor contribution to the electrostatic potential. Even more disturbing is the apparent irreconcilability of our result with those of others[1,5,21-23] who have obtained reasonable results for anharmonic properties in the alkali halides using parameters λ and ρ derived solely from harmonic models based on the phonon frequencies.

Some authors[2,21] have emphasized that quartic anharmonicity, particularly at temperatures above the Debye temperature and for crystals with a substantial frequency gap between the optic and acoustic branches, may give a contribution comparable to or even greater than that of cubic anharmonicity. KI at room temperature seems to be a good candidate in which to look for quartic contributions. As we have pointed out, quartic anharmonicity is necessary to account for our values of k above 175 cm^{-1}, but here k is very small in magnitude so that a quartic term would not necessarily give a substantial enough contribution to influence the optical constants in other regions. Furthermore, this would only decrease the value of A_3 required to give agreement with our experiment. Such

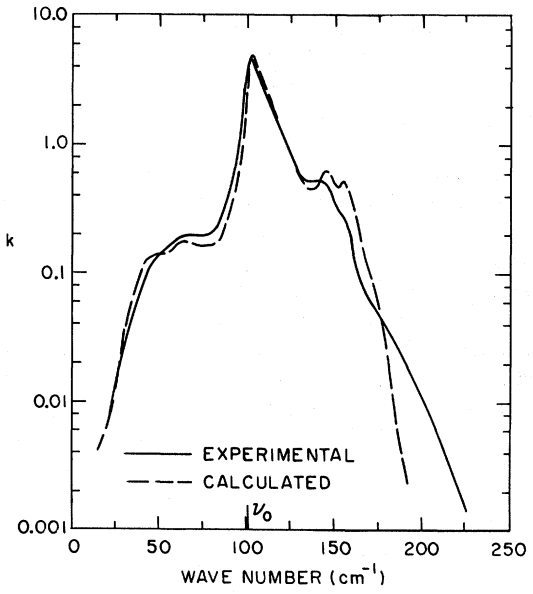

FIG. 8. Experimental and calculated extinction coefficient for KI.

a contribution, however, would be expected to cause further spreading of the peaks in the wings of the absorption region, causing better agreement with experiment in this respect.

It is possible that a more refined model may be necessary in order to more meaningfully measure the anharmonic constants and the relative effects of cubic and quartic anharmonicity on the optical properties. Such a model should include forces other than central forces between nearest-neighbor ions. No serious attempt has yet been made to include the effects of electrostatic and ionic depolarization forces in an anharmonic calculation. It would be far more desirable, however, to be able to obtain the anharmonic constants from measurable quantities which are more simply related to these constants.

A few words seem in order with regard to the magnitudes of the high- and low-frequency dielectric constants $\epsilon(\infty)$ and $\epsilon(0)$. For $\epsilon(\infty)$ we have used the square of the experimental asymptotic high-frequency index of refraction. Since the shell model includes the polarizabilities of the ions, it can be used to calculate a value for $\epsilon(\infty)$. Dolling *et al.*[5] find $\epsilon(\infty)=2.41$, substantially lower than the experimental value of 2.69.[10] Comparing the Cowley susceptibility formula[1] with our Eq. (5), we should have

$$[\epsilon(0)-\epsilon(\infty)][\omega_0^2+2\omega_0\Delta(0j_0,0)]=4\pi Z_T^2/v_c\,, \quad (18)$$

where v_c is the volume of the unit cell $2r_0^3$, and Z_T is the effective ionic charge acted upon by the macroscopic electric field in the long-wavelength limit. For the shell model used here we find that $Z_T = 1.034e$, where e is the electronic charge. Using the shell-model value of $\epsilon(\infty)$, we find[9] $\epsilon(0)=4.43$, again substantially below the experimental value. The ratio $\epsilon(0)/\epsilon(\infty)$ in both cases is very near 1.86. This is no coincidence in view of the Lyddane-Sachs-Teller relation[17] which expresses this ratio in terms of the frequencies of the LO(0) and TO(0) modes of vibration, for the case of a purely harmonic model, where the self-energy contribution vanishes. The rather large error in these dielectric values contributes to the lack of confidence in the ability of this shell model for KI to give the force parameters λ and ρ correctly.

VI. CONCLUSION

The optical constants of KI were calculated on the basis of a model which includes cubic anharmonicity in a central nearest-neighbor potential $\Phi(r)$. Adjustment of the third derivative $\Phi'''(r_0)$ led to good agreement with experiment in the spectral region where three-phonon interactions are allowed by energy conservation to contribute to the self-energy. The value of the potential-energy parameter so obtained is roughly half that calculated from the shell model of Dolling *et al.*,[5] using the expression $\Phi(r)=\lambda e^{-r/\rho}$. Although the validity of such a calculation was questioned, the deficiencies in our model were also pointed out.

ACKNOWLEDGMENTS

The authors wish to acknowledge the valuable advice and assistance of K. Johnson, R. Sanderson, R. Ulrich, and R. Gillespie. We wish to thank G. Dolling for valuable correspondence.

---

†Work partially supported by the U. S. Air Force Cambridge Research Laboratories.

*Present address: Honeywell Research Center, Hopkins, Minn. 55343.

[1]R. A. Cowley, Advan. Phys. 12, 421 (1963).

[2]L. É. Gurevich and I. P. Ipatova, Zh. Eksperim. i Teor. Fiz. 45, 231 (1963) [Sov. Phys. JETP 18, 162 (1964)].

[3]R. F. Wallis, I. P. Ipatova, and A. A. Maradudin, Fiz. Tverd. Tela 8, 443 (1966) [Sov. Phys. Solid State 8, 850 (1966)].

[4]K. W. Johnson and E. E. Bell, Phys. Rev. 187, 1044 (1969).

[5]G. Dolling, R. A. Cowley, C. Schittenhelm, and I. M. Thorson, Phys. Rev. 147, 577 (1966).

[6]E. E. Bell, Infrared Phys. 6, 57 (1966).

[7]E. E. Russell and E. E. Bell, Infrared Phys. 6, 75 (1966).

[8]E. W. Kellerman, Phil. Trans. Roy. Soc. London A238, 513 (1940).

[9]J. I. Berg, Ph. D. dissertation (The Ohio State University, 1969) (unpublished).

[10]K. Korth, Z. Physik 84, 677 (1933).

[11]A. Hadni, J. Claudel, G. Moriot, and P. Strimer, Appl. Opt. 7, 161 (1968).

[12]S. Hassuhl, Z. Naturforsch. 12a, 445 (1957).

[13]K. Højendahl, Kgl. Danske Videnskab. Selskab, Mat.-Fys. Medd. 16, 59 (1938).

[14]B. W. Jones, Phil. Mag. 16, 1085 (1967).

[15]R. D. Lowndes and D. H. Martin, Proc. Roy. Soc. (London) A308, 473 (1969).

[16]A. A. Maradudin, E. W. Montroll, and G. H. Weiss, *Theory of Lattice Dynamics in the Harmonic Approximation* (Academic, New York, 1963).

[17]M. Born and K. Huang, *Dynamical Theory of Crystal Lattices* (Clarendon, Oxford, 1954).

[18]A. A. Maradudin and A. E. Fein, Phys. Rev. 128, 2589 (1962).

[19]A. D. B. Woods, W. Cochran, and B. N. Brockhouse, Phys. Rev. 119, 980 (1960).

[20]R. A. Cowley, W. Cochran, B. N. Brockhouse, and A. D. B. Woods, Phys. Rev. 131, 1030 (1963).

[21]I. P. Ipatova, A. A. Maradudin, and R. F. Wallis, Phys. Rev. 155, 882 (1967).

[22]E. R. Cowley and R. A. Cowley, Proc. Roy. Soc. (London) A287, 259 (1965).

[23]E. R. Cowley and R. A. Cowley, Proc. Roy. Soc. (London) A292, 209 (1966).